ORIGINAL RESEARCH

Histone Acetyltransferase p300 Inhibitor Improves Coronary Flow Reserve in SIRT3 (Sirtuin 3) Knockout Mice

Han Su, MD; Heng Zeng, MD; Xiaochen He, PhD; Shai-Hong Zhu, MD; Jian-Xiong Chen (ID), MD

BACKGROUND: Coronary microvascular dysfunction is common in patients of myocardial infarction with non-obstructive coronary artery disease. Coronary flow reserve (CFR) reflects coronary microvascular function and is a powerful independent index of coronary microvascular dysfunction and heart failure. Our previous studies showed that knockout of SIRT3 (Sirtuin 3) decreased CFR and caused a diastolic dysfunction. Few studies focus on the treatment of impaired CFR and heart failure. In the present study, we explored the role of C646, a histone acetyltransferase p300 inhibitor, in regulating CFR and cardiac remodeling in SIRT3 knockout (SIRT3KO) mice.

METHODS AND RESULTS: After treating with C646 for 14 days, CFR, pulse-wave velocity, and cardiac function were measured in SIRT3KO mice. SIRT3KO mice treated with C646 showed a significant improvement of CFR, pulse-wave velocity, ejection fraction, and fractional shortening. Treatment with C646 reversed pre-existing cardiac fibrosis, hypertrophy, and capillary rarefaction in SIRT3KO mice. Mechanistically, knockout of Sirtuin 3 resulted in significant increases in p300 expression and H3K56 acetylation. Treatment with C646 significantly reduced levels of p300 and H3K56 acetylation in SIRT3KO mice. Furthermore, treatment with C646 increased endothelial nitric oxide synthase expression and reduced arginase II expression and activity. The expression of NF-κB (nuclear factor kappa-light-chain-enhancer of activated B cells) and VCAM-1 (vascular cell adhesion molecule 1) was also significantly suppressed by C646 treatment in SIRT3KO mice.

CONCLUSIONS: C646 treatment attenuated p300 and H3K56 acetylation and improved arterial stiffness and CFR via improvement of endothelial cell (EC) dysfunction and suppression of NF-κB.

Key Words: C646 ■ coronary flow reserve ■ coronary microvascular disease ■ H3K56 acetylation ■ p300

Coronary artery disease is the leading cause of death in the United States and in developed countries. In patients of myocardial infarction with nonobstructive coronary artery disease, coronary microvascular dysfunction (CMD) is common as evidenced by a reduction in coronary flow reserve (CFR). CFR is the ratio of peak blood flow to basal blood flow, indicating the structural and functional conditions of coronary microcirculation. CFR is an essential predictor of cardiovascular diseases such as diastolic dysfunction and heart failure with preserved ejection fraction.[1–4] An impaired CFR is also strongly correlated with higher mortality in patients of hypertension and metabolic diseases. Many pathological conditions such as diabetes mellitus and hypertension are associated with decreased CFR.[1–3] Importantly, preserved CFR in diabetic patients reduces the number of cardiac events to the levels seen in nondiabetic controls.[5] Therefore, strategies to restore CFR or improve CMD have the promise to reduce higher mortality in heart failure. Currently, because of a lack of mechanistic studies, there are no proven treatments for CMD. The mechanisms related to CMD are unclear, but endothelial dysfunction and microvascular rarefaction are suggested

Correspondence to: Jian-Xiong Chen, MD, Department of Pharmacology and Toxicology, University of Mississippi Medical Center, 2500 North State Street, Jackson, MS, 39216, E-mail: jchen3@umc.edu or Heng Zeng, MD, Department of Pharmacology and Toxicology, University of Mississippi Medical Center, 2500 North State Street, Jackson, MS, 39216, E-mail: hzeng@umc.edu

CLINICAL PERSPECTIVE

What Is New?

- SIRT3 (Sirtuin 3) was resident in the nuclei and knockout of SIRT3-increased p300 and H3K56 acetylation.
- Treatment with a histone acetyltransferase p300 inhibitor (C646) attenuated p300 and H3K56 acetylation and revised the pre-existing impairments of coronary flow reserve and cardiac function in SIRT3 knockout mice.
- C646 may alleviate coronary microvascular dysfunction via rebalancing arginase/endothelial nitric oxide synthase and attenuate cardiac remodeling via suppressing TLR-4/IRAK-4/MyD88–mediated NF-κB.

What Are the Clinical Implications?

- The prevalence of coronary microvascular dysfunction in myocardial infarction with nonobstructive coronary artery disease, defined as a reduced coronary flow reserve, is increasing at an alarming rate, and so far there is no proven treatments for coronary microvascular dysfunction because of the incomplete understanding of the underlying mechanisms.
- Our present study provides a novel role of the histone acetyltransferase p300 inhibitor on coronary microvascular dysfunction and cardiac remodeling and will create a new platform for drug discovery for the nonobstructive coronary artery disease in aged populations.

Nonstandard Abbreviations and Acronyms

CFR	coronary flow reserve
CMD	coronary microvascular dysfunction
ECs	endothelial cells
eNOS	endothelial nitric oxide synthase
HAT	histone acetyltransferase
PWV	pulse-wave velocity
ROS	reactive oxygen species

as 2 important contributors to reduced CFR.[2,3,6–10] Nevertheless, it is urgent to further understanding in the pathophysiological mechanisms of CMD.

SIRT3 (Sirtuin 3), which is a class III histone deacetylase, is responsible for many cellular functions such as metabolic homeostasis, oxidative stress, and apoptosis.[11–14] SIRT3 is well known to have a critical role in cardiac remodeling and heart failure.[15,16] Patients with failing hearts have a reduced level of SIRT3 with excessive cardiac fibrosis.[17] P300 is a histone acetyltransferase (HAT) regulating the acetylation of proteins responsible for a variety of cellular processes such as proliferation, differentiation, and apoptosis.[18] Although SIRT3 was originally identified in mitochondria, few studies also showed SIRT3 in the nucleus where it functions as a histone deacetylase and modulates the expression of stress-related and nuclear-encoded genes.[19,20] Accumulating evidence suggests that the counterbalancing of histone deacetylase and HATs plays an essential role in cardiovascular diseases.[21,22] The p300 HAT has been shown to acetylate histone H3K56 in vitro and in vivo, whereas SIRT3 deacetylates H3K56Ac in vivo, which is one of the core domain histone modifications, having its function in DNA damage response.[23] Our previous studies have revealed that the deletion of SIRT3 in endothelial cells (ECs) causes cardiac remodeling, diastolic dysfunction, and reduced CFR via shifting endothelial metabolism and angiogenesis.[13,15,16,24–26] Studies have showed that p300 HAT was associated with cardiac remodeling.[27–30] Recently, C646, as a p300 HAT inhibitor, has been shown to reverse hypertension-induced fibrosis and hypertrophy.[31] Hypertrophy and fibrosis are known to be correlated with reduced CFR.[32–35] A previous study revealed a counterinteraction of p300 and SIRT3 in skp2-mediating oncogenic function.[36] So far, the association between SIRT3 and p300 in cardiac remodeling and CFR and its underlying mechanisms still remain elusive. Therefore, we investigated the underlying mechanisms of a p300 inhibitor (C646) on cardiac remodeling as well as its direct effect on impaired CFR in SIRT3 knockout (SIRT3KO) mice.

In the present study, we aimed to explore the mechanisms of the acetyltransferase p300 inhibitor C646 in regulating CFR, pulse-wave velocity (PWV), and cardiac remodeling in SIRT3KO mice. Using immunofluorescence, we found that the SIRT3 was located in the nucleus in cultured mouse ECs. Knockout of SIRT3 significantly increased p300 expression and H3K56 acetylation in vivo. Our data further demonstrated that C646 treatment significantly improved arterial stiffness, CFR, and cardiac function in SIRT3KO mice. Moreover, pre-existing cardiac remodeling such as fibrosis, hypertrophy, and microvascular rarefaction was reversed by C646 treatment in the SIRT3KO mice. Mechanistically, C646 treatment attenuated levels of p300 and H3K56 acetylation together with increased endothelial nitric oxide synthase (eNOS) expression and reduced arginase II and activity in SIRT3KO mice. Treatment with C646 suppressed NF-κB (nuclear factor kappa-light-chain-enhancer of activated B cells) and coronary artery VCAM-1 (vascular cell adhesion molecule 1) expression in SIRT3KO mice, indicating a reduction of vascular inflammation. Our data suggest that C646 may be a novel agent for the treatment of CMD.

METHODS

The authors declare that all supporting data are available within the article.

All procedures conformed to the Institute for Laboratory Animal Research *Guide for the Care and Use of Laboratory Animals*. It was also approved by the Animal Care and Use Committee of the University of Mississippi Medical Center (Protocol Identification 1564). The investigation conformed to the National Institutes of Health (Bethesda, MD) *Guide for the Care and Use of Laboratory Animals* (National Institutes of Health Publication No. 85-23, revised 1996).

Experimental Animal Model and Treatment

Wild-type (WT) control and SIRT3KO (Stock No. 012755) mice were originally obtained from Jackson Laboratory (Bar Harbor, ME) and bred in our laboratory. The experimental mice were fed normal chow and water. Male mice at age of 4 to 7 months having similar impairments of CFR and cardiac function were chosen to perform experiments. SIRT3KO mice were treated with saline and C646 (1 µg/gm; Millipore Sigma, Burlington, MA) every day for 14 days by intraperitoneal injection. Our pilot study showed that young female mice aged 4 to 7 months did not exhibit impairment of CFR and cardiac function; therefore, young female mice were excluded from our study.

Cell Culture and Treatment

Mouse aortic ECs were isolated and cultured from the thoracic aortas of SIRT3KO mice as previously described.[37,38] The H9C2 cell lines were obtained from American Type Culture Collection (Manassas, VA). Standard DMEM basic was used for the mouse aortic ECs and H9C2 cell culture. These cells were maintained at 37°C and 5% CO_2.[39] ECs and H9C2 cells were treated with and without C646 (1–3 µmol/L) for 24 hours. Proteins were collected and used for Western blots.

Echocardiography and Aortic Stiffness

After administration of C646 for 14 days, we measured transthoracic echocardiograms in WT, SIRT3KO, and SIRT3KO mice+C646 by using the Vevo3100 Imaging System (VisualSonics Inc, Toronto, ON, Canada). The cine loop of the left proximal coronary artery was visualized in a modified parasternal left ventricle short-axis view by inhalation of 1% isoflurane for baseline and 2.5% isoflurane for hyperemic conditions for CFR. The ratio of peak blood flow velocity during hyperemia to the peak blood flow velocity at baseline was used to calculate the CFR. High-frequency ultrasound imaging software (VisualSonics Inc) was used to analyze

M-mode cine loops for the assessment of myocardial parameters and cardiac functions of the left ventricle including ejection fraction and fractional shortening.[13,15,16,24,40] Arterial stiffness was measured with noninvasive Doppler ultrasound. The time difference between the peak aortic flow at 2 distinct locations of known distance in the aorta was measured to estimate PWV. PWV was calculated using the following equation: PWV = (distance between probes/[Δtime t_1 − Δtime t_2]).

Histological and Immunofluorescence Analysis

Some heart tissues were fixed with neutral-buffered 10% formalin solution (SF93–20; Fisher Scientific, Pittsburgh, PA). The other tissues were embedded in frozen OCT compound (4585; Fisher Health Care, Houston, TX). The paraffin and frozen sections were prepared with 10 µm in thickness. We prepared all of the tissues under the same conditions. Paraffin sections were stained with Masson's trichrome staining and hematoxylin–eosin. Some frozen sections were stained with dihydroethidium staining for reactive oxygen species (ROS) measurement. Some frozen sections were immune stained with VCAM-1 (1:150; Cell Signaling, Danvers, MA). Isolectin B4 (frozen section) was performed to measure ECs (1:150; Invitrogen, Carlsbad, CA) and capillary density. Images were obtained with a Nikon microscope, Nikon digital camera, and Nikon software (Nikon, Tokyo, Japan). Seven random microscopic fields were chosen for analysis with image analysis software (Image J, National Institutes of Health).

Western Blot Analysis

Mouse left ventricle tissues, H9C2 cells, and ECs were collected and sonicated in lysis buffer. The homogenates were centrifuged at 16 000*g* at 4°C for 15 minutes. The protein concentrations were analyzed with a BCA protein assay kit (Pierce Co, Rockford, IL). An aliquot (30 µg for heart tissues and 25 µg for cells) of protein samples was separated by 10% SDS-PAGE gel and transferred to a polyvinylidene difluoride membrane. The membranes were blocked with 5% dry milk in Tris-buffered saline and incubated with the following primary antibodies overnight: p300 (1:1000; Cell Signaling), acetyl-histone H3 (lys56) (H3K56ac, 1:1000; Cell Signaling), total lysine acetylation (1:1000; Cell Signaling), β-MHC (β-myosin heavy chain; 1:1000; Abcam, Cambridge, MA), arginase I and II (1:1000; Novus Bio, Littleton, CO), NF-κB, TLR-4 (toll-like receptor 4), MyD88 (myeloid differentiation primary response 88; 1:1000; Santa Cruz, CA), eNOS (1:1000; BD Transduction, San Jose, CA), VCAM-1 and IRAK-4 (interleukin-1 receptor-associated kinase 4; 1:1000;

Cell Signaling). After washing, the membranes were incubated for 2 hours with an anti-rabbit or anti-mouse secondary antibody coupled to horseradish peroxidase (1:5000; Santa Cruz). Densitometric analyses were performed with image acquisition and analysis software (Bio-Rad, Hercules, CA).

Arginase Activity Assay

An arginase activity assay kit was acquired from Sigma-Aldrich (St. Louis, MO). Protein samples were extracted from heart tissues. Urea standard working solution (50 µL), distilled water (50 µL), and a protein sample (40 µL for sample well and 40 µL for sample blank well) were added into a 96-well plate. A 5× substrate buffer (10 µL) was added into every sample well to start arginase activity. After incubation of these mixtures at 37°C for 2 hours, a urea reagent was added into all wells (urea standard well, distilled water well, sample well, and sample blank well) to stop the reaction. The 5× substrate buffer (10 µL) was then added to the sample blank well. After incubation at 37°C for 1 hour, the absorbance was measured at 430 nm.

Immunofluorescence

Isolated ECs from WT mice were washed with PBS and fixed in 4% formaldehyde for 10 minutes at room temperature and then incubated with 5% normal goat serum in 0.3% Triton X-100/PBS for 1 hour to permeabilize the cells and block nonspecific protein–protein interaction. The cells were then incubated with the rabbit anti-SIRT3 antibody (Abcam, ab 86671, 1:100) in 1% BSA in 0.3% Triton X-100/PBS overnight at +4°C, followed by secondary Cy™3 donkey anti-rabbit antibody (1:200; No. 711-165-152; Jackson Immunoresearch Laboratories, West Grove, PA) for 1 hour; 4′,6-diamidino-2-phenylindole was used to stain the cell nuclei.

Statistical Analysis

Data are presented as mean±SEM. The assumption of normality in both comparison groups were determined by normality and long-normality tests. Statistical significance was determined using the Student unpaired 2-tailed t-test for comparisons between 2 groups and 1-way or 2-way ANOVA followed by a Tukey post hoc test for multiple comparisons using GraphPad Prism 8.1.1 software (GraphPad Software, La Jolla, CA). $P<0.05$ was considered statistically significant.

RESULTS

C646 Improved CFR, Arterial Stiffness, and Cardiac Performance in SIRT3KO Mice

Measurement of coronary microvascular function studies showed that CFR was significantly reduced in SIRT3KO mice compared with that of WT mice, whereas treatment with C646 for 14 days significantly enhanced CFR levels in the SIRT3KO mice (Figure 1A). Arterial stiffness measurement revealed an increased PWV in the SIRT3KO mice, indicating that knockout of SIRT3 led to increased stiffness of the artery. Treatment with C646 significantly blunted this increase in the SIRT3KO mice (Figure 1B). Moreover, C646 treatment significantly improved cardiac performance as evidenced by an increased ejection fraction and fractional shortening (Figure 1C) and a reduced systolic volume in the SIRT3KO mice (Table).

## C646 Reversed Pre-existing Cardiac Remodeling in SIRT3KO Mice

Masson staining showed that knockout of SIRT3 resulted in increased interstitial fibrosis, whereas cardiac fibrosis in the SIRT3KO mice with C646 treatment was significantly decreased. The coronary artery Wall-lumen ratio was higher in the SIRT3KO mice compared with the WT mice; however, no significant difference was found between the SIRT3KO mice and SIRT3KO mice+C646 (Figure 2A). Moreover, hematoxylin–eosin staining revealed that C646 treatment significantly ameliorated a SIRT3KO-induced increase in cardiomyocyte size, which was further confirmed by decreased heart weight:tibia length and β-MHC expression in SIRT3KO mice+C646 (Figure 2B). Also, knockout of SIRT3 resulted in a dramatic reduction of myocardial capillary density, whereas capillary density was significantly increased by treatment with C646 for 14 days (Figure 2C).

C646 Treatment Increased eNOS Expression and Reduced ROS Formation in SIRT3KO Mice

Western blot analysis revealed that knockout of SIRT3 decreased expression of eNOS, whereas treatment with C646 significantly blunted this down-regulation

Figure 1. C646 treatment improved coronary microvascular dysfunction and cardiac dysfunction in SIRT3KO mice.
A, Representative images of coronary flow reserve recording in mouse coronary artery. Coronary flow reserve was significantly impaired in the SIRT3KO mice. C646 treatment significantly improved coronary flow reserve in the SIRT3KO mice (n=5 mice). Mean±SEM, *$P<0.05$. **B**, Representative images of PWV recording in mouse aorta. PWV was significantly elevated in the SIRT3KO mice. Increased PWV was significantly attenuated by C646 treatment in the SIRT3KO mice (n=6 mice). Mean±SEM; *$P<0.05$, **$P<0.01$. **C**, Representative images of M-mode in a mouse heart. Knockout of SIRT3 reduced levels of EF% and FS% compared with WT mice. Treatment with C646 significantly reversed these changes (n=6 mice), Mean±SEM; *$P<0.05$, ***$P<0.001$. EF indicates ejection fraction; FS, fractional shortening; PWV, pulse-wave velocity; SIRT3, sirtuin 3; SIRT3KO, SIRT3 knockout; and WT, wild type.
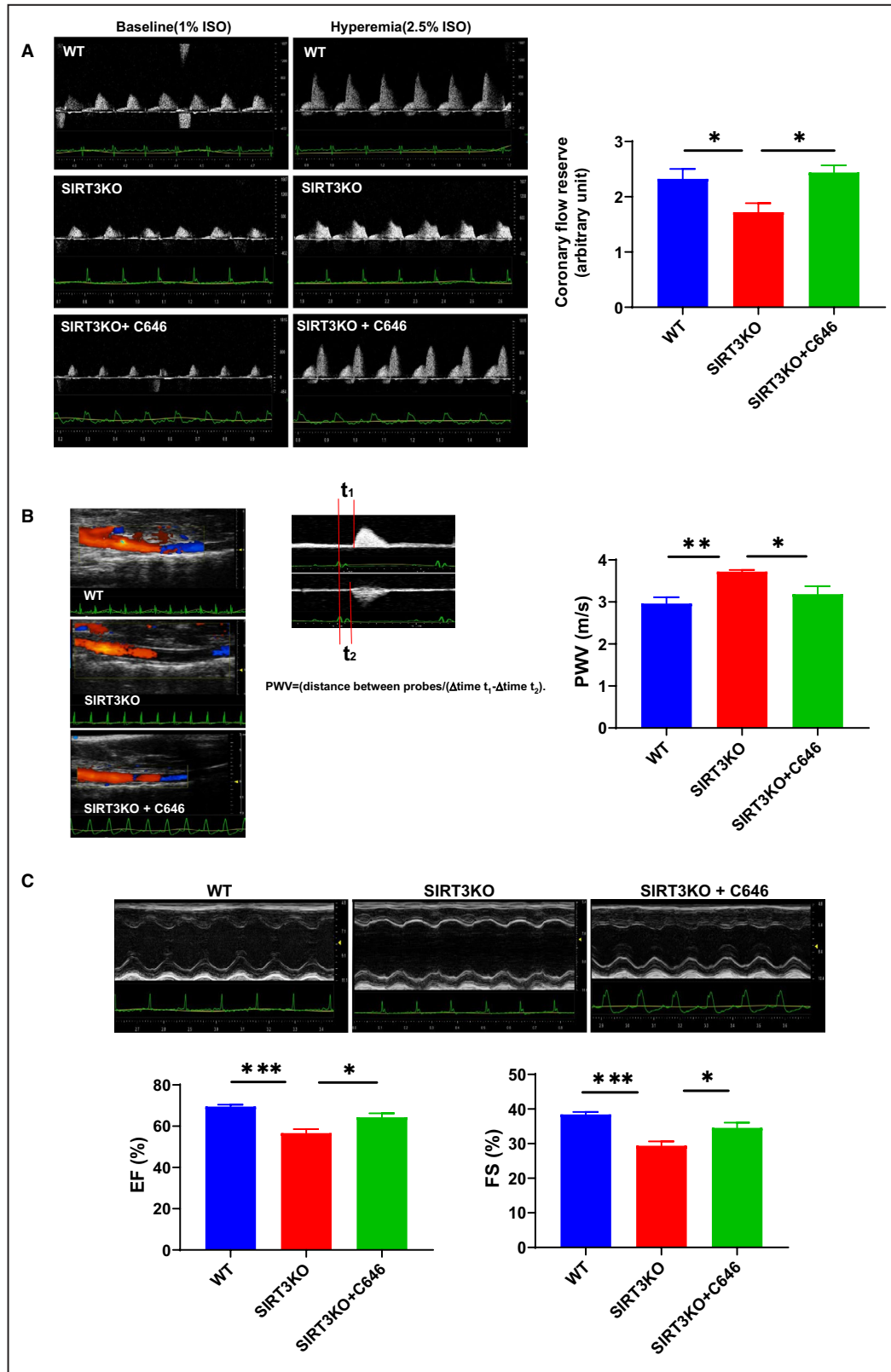
(Figure 3A). Knockout of SIRT3 increased ROS formation in the mouse hearts. SIRT3KO-mediated increased ROS formation was significantly reversed by C646 treatment (Figure 3B).

C646 Suppressed Arginase II Expression and Activity in SIRT3KO Mice

Knockout of SIRT3 significantly increased arginase activity in the mouse hearts. SIRT3KO-induced

Table 1. Measurement of Heart Rate and Cardiac Function by Echocardiography

	Control (n=7)	SIRT3KO (n=5)	SIRT3KO+C646 (n=6)
Heart rate, bpm	458±3	452±2	451±5
Diameter, s, mm	2.29±0.10	2.91±0.11*	2.49±0.12
Diameter, d, mm	3.72±0.14	4.12±0.11	3.81±0.16
Volume, s, μL	18.37±2.15	32.94±3.05*	22.59±2.74#
Volume, d, μL	59.49±5.35	75.56±4.67	63.02±6.15
Stroke volume, μL	41.12±3.29	42.62±2.21	40.43±3.93
Cardiac output, mL/min	18.83±1.51	19.27±0.99	18.16±1.63
Left ventricle mass, mg	95.17±8.07	85.12±5.84	105.22±9.57

One-way ANOVA, followed by the Tukey post hoc test. Data are presented as mean±SD. d indicates diastolic; s, systolic; SIRT3, sirtuin 3; and SIRT3KO, SIRT3 knockout.

*$P<0.05$ vs control.

#$P<0.05$ vs SIRT3KO.

arginase activity was inhibited by C646 treatment (Figure 4A). Western blot analysis showed that there was no significant difference of arginase I expression among WT mice, SIRT3KO mice, or SIRT3KO mice+C646 (Figure 4B). In contrast, arginase II expression was up-regulated in the SIRT3KO mice. Treatment with C646 resulted in significant suppression of arginase II expression in the SIRT3KO mice (Figure 4C).

C646 Treatment Reduced VCAM-1 Expression in SIRT3KO Mice

Western blot analysis showed that VCAM-1 levels were significantly increased in the SIRT3KO mice. C646 treatment suppressed VCAM-1 expression in the SIRT3KO mice (Figure 5A). An immunostaining study further showed that VCAM-1 expression was increased in the coronary artery of SIRT3KO mice, whereas C646 treatment reversed elevated levels of VCAM-1 in the coronary artery (Figure 5B). In addition, an immunostaining study showed that the majority of VCAM-1 positive staining was located in the ECs of mouse hearts (Figure 5B).

In vitro exposure of cultured ECs to C646 for 24 hours resulted in a significant increase in eNOS expression at a concentration of 3 μmol/L. Furthermore, C646 treatment significantly reduced arginase II expression in a dose-dependent manner. Treatment of ECs with C646 also suppressed VCAM-1 expression at a concentration of 3 μmol/L (Figure 5C).

C646 Ameliorated NF-κB Expression in SIRT3KO Mice

The basal levels of NF-κB, TLR-4, MyD88, and IRAK-4 were significantly up-regulated in the hearts of SIRT3KO mice. Treatment with C646 blunted the up-regulation expression of NF-κB, TLR-4, MyD88, and IRAK-4 in the SIRT3KO mice (Figure 6A). In the cultured H9C2

cell lines, C646 (3 μmol/L) treatment significantly suppressed the basal levels of NF-κB, TLR-4, MyD88, and IRAK-4 (Figure 6B).

Effects of C646 on SIRT3KO-Mediated p300 Expression and H3K56 Acetylation

To study whether SIRT3 were located in the nucleus, we colocalized SIRT3 with the nuclei marker 4′,6-di-amidino-2-phenylindole using immunofluorescence in the cultured ECs isolated from WT mice. As shown in Figure 6C, the SIRT3 antibodies recognized a protein that resided in the nucleus that was colocalized with the blue 4′,6-diamidino-2-phenylindole regions. Western blot analysis showed that the levels of p300 and H3K56 acetylation were significantly increased in the hearts of the SIRT3KO mice (Figure 6D and 6E). Treatment with C646 significantly reduced p300 expression and acetylated K3K56 levels in the SIRT3KO mice (Figure 6D and 6E). The total lysine acetylation levels were significantly increased in the hearts of the SIRT3KO mice; however, C646 treatment had little effect on total acetylated lysine levels in the hearts of the SIRT3KO mice (Figure 6F).

DISCUSSION

In the present study, we demonstrated that C646, the acetyltransferase p300 inhibitor, alleviated SIRT3KO-induced cardiac remodeling including cardiac fibrosis, hypertrophy, and capillaries rarefaction. This was accompanied by an improvement of CFR and arterial stiffness. Knockout of SIRT3 significantly increased p300 expression and H3K56 acetylation. Knockout of SIRT3 resulted in an imbalanced arginase/eNOS in favor of arginase and increased arginase activity. Treatment with C646 blunted p300 and H3K56 acetylation in the hearts of SIRT3KO mice. Treatment with C646 rebalanced arginase/eNOS and reduced
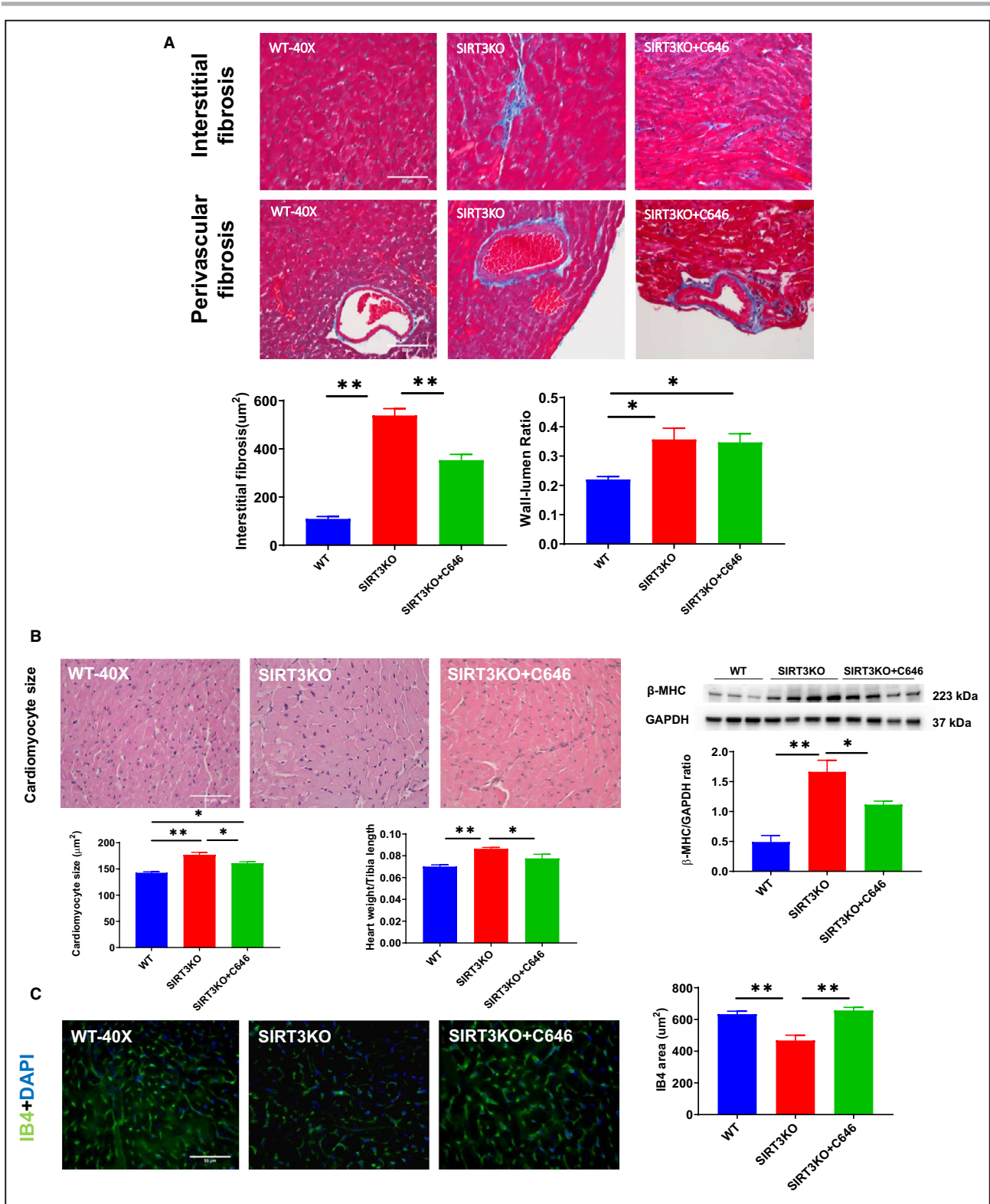
Figure 2.   C646 reversed pre-existing cardiac remodeling in SIRT3KO mice.
A, Interstitial and perivascular fibrosis were increased in the SIRT3KO mice (n=3 mice) compared with WT mice (n=3 mice). C646 treatment suppressed increased interstitial and perivascular fibrosis in the SIRT3KO mice significantly (n=3 mice). Mean±SEM; *P<0.05, **P<0.01. **B**, Knockout of SIRT3 resulted in increased cardiomyocyte size, heart weight:tibia length ratio, and β-MHC expression in the heart (n=3 mice), whereas treatment with C646 reversed these alterations (n=3 mice). Mean±SEM; *P<0.05, **P<0.01. **C**, Capillary density was reduced in the SIRT3KO mice (n=3 mice) in comparison with WT mice (n=3 mice). This reduction in capillary density was reversed by treatment with C646 (n=3 mice). Mean±SEM; **P<0.01. βMHC indicates β-myosin heavy chain; DAPI, 4′,6-diamidino-2-phenylindole; IB4, isolectin B4; SIRT3, sirtuin 3; SIRT3KO, SIRT3 knockout; and WT, wild type.
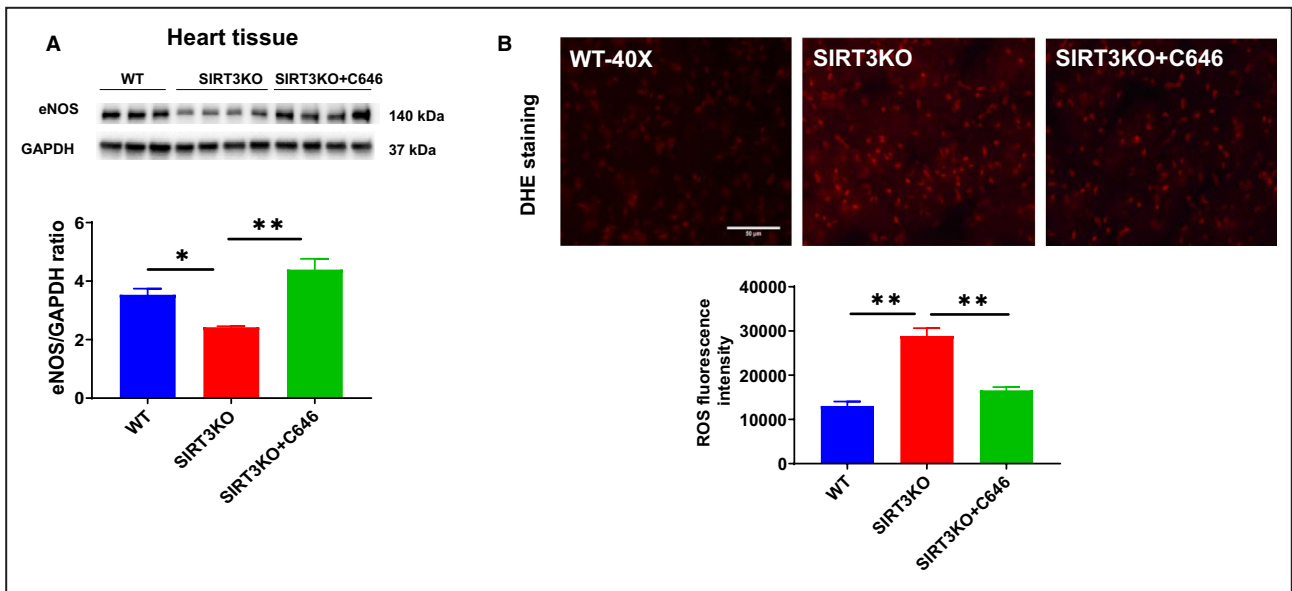
Figure 3. C646 improved eNOS and oxidative stress in SIRT3KO mice.
A, Treatment with C646 reversed reduction of eNOS levels in the SIRT3KO mice (n=4 mice). Mean±SEM; *P<0.05, **P<0.01. **B**, By DHE staining, ROS formation was enhanced in the SIRT3KO mice (n=3 mice) compared with the WT mice (n=3 mice). This enhancement was suppressed by treatment with C646 (n=3 mice). Mean±SEM; **P<0.01. DHE indicates dihydroethidium; eNOS, endothelial nitric oxide synthase; ROS, reactive oxygen species; SIRT3, sirtuin 3; SIRT3KO, SIRT3 knockout; and WT, wild type.

arginase activity. In addition, C646 suppressed expression of NF-κB and VCAM-1. Our data suggest that treatment with C646 reduced p300 expression and H3K56 acetylation and improves CFR and cardiac function by the mechanisms involved in reversing arginase II/eNOS imbalance-induced microvascular dysfunction and attenuating NF-κB-mediated inflammatory responses.

In this study, we demonstrated that treatment with C646 significantly increased CFR in the SIRT3KO mice. CFR, as a predictor of cardiovascular diseases, is associated with coronary microvascular diseases,[1–5] and improving CFR by C646 may partly explain the alleviation of cardiac dysfunction in the SIRT3KO mice. We aim to investigate the specific mechanisms of the improvement of CFR with C646. Because CFR reflects
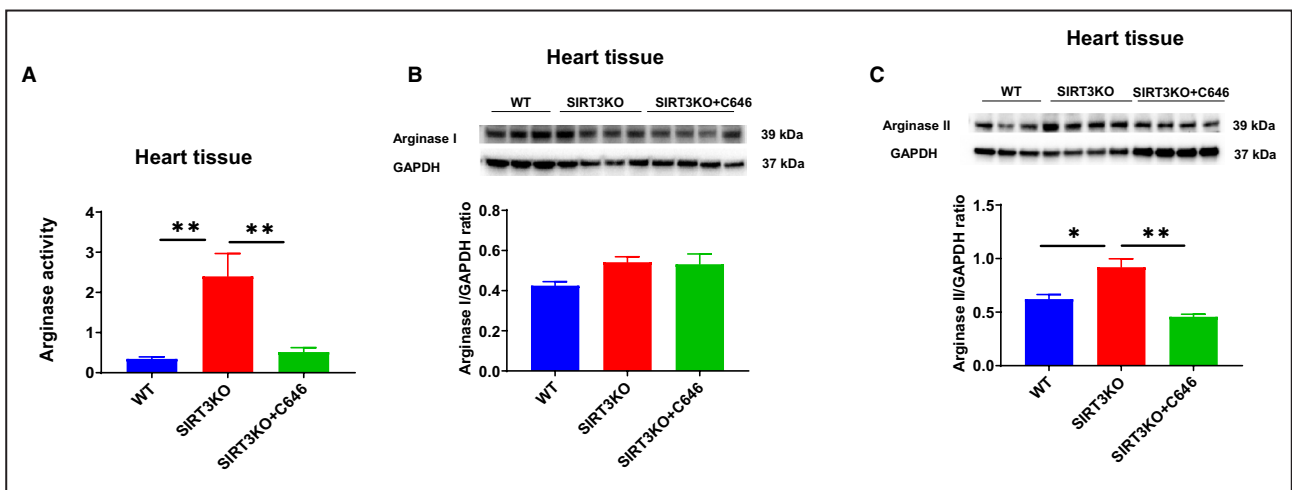
Figure 4. C646 treatment-inhibited arginase II expression and arginase activity in SIRT3KO mice.
A, Arginase activity was enhanced in the SIRT3KO mice (n=5 mice) in comparison with the WT mice (n=5 mice). Treatment with C646 inhibited arginase activity significantly (n=5 mice). Mean±SEM; **P<0.01. **B**, No difference in arginase I expression was found among the WT mice (n=3 mice), SIRT3KO mice (n=4 mice), or SIRT3KO mice+C646 (n=4 mice). **C**, Treatment with C646 reversed the increased arginase II expression in the SIRT3KO mice (n=4 mice). Mean±SEM; *P<0.05, **P<0.01. SIRT3 indicates sirtuin 3; SIRT3KO, SIRT3 knockout; and WT, wild type.
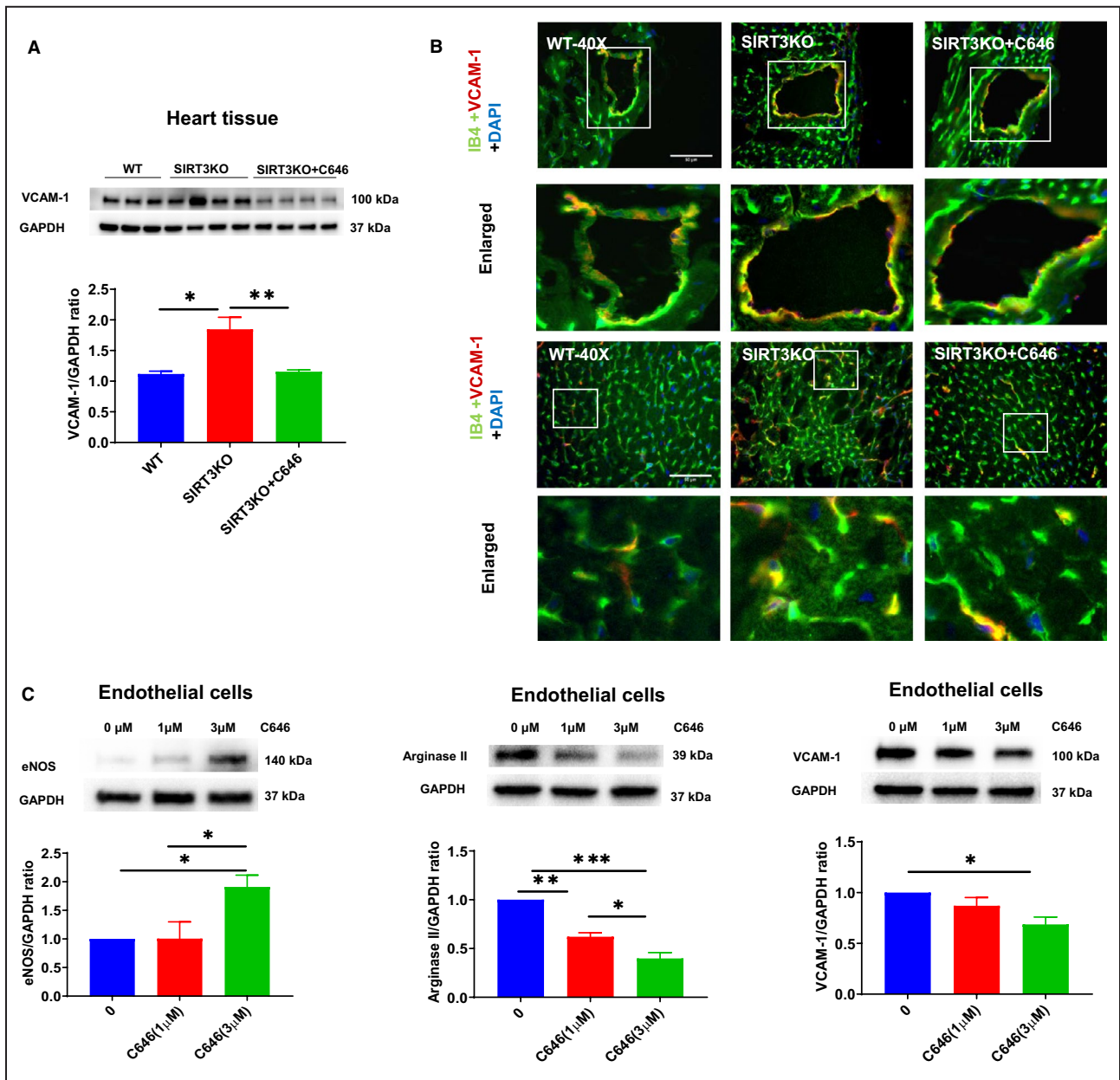
Figure 5. Treatment with C646 suppressed VCAM-1 expression in SIRT3KO mice.

A, Knockout of SIRT3 increased VCAM-1 expression (n=4 mice), whereas C646 treatment inhibited VCAM-1 expression significantly (n=4 mice). Mean±SEM; *$P<0.05$, **$P<0.01$. **B**, By costaining IB4 and VCAM-1, we found that VCAM-1 expression was colocalized with endothelial cells. Knockout of SIRT3 increased the number of IB4+/VCAM-1+ cells (n=3 mice), and treatment with C646 reversed this increase (n=3 mice). Similarly, enhanced expression of VCAM-1 in the endothelial cells of the coronary artery was found in SIRT3KO mice compared with WT mice. Treatment with C646 suppressed the up-regulation of VCAM-1 in the endothelial cells of the coronary artery. **C**, C646 increased eNOS and reduced arginase II and VCAM-1 expression in the cultured endothelial cells. Exposure of cultured endothelial cells with C646 (3 μmol/L) significantly increased eNOS expression (n=3 mice). Mean±SEM; *$P<0.05$. Treatment with C646 resulted in a dose-dependent reduction of arginase II expression in the cultured endothelial cells (n=3 mice). Mean±SEM; *$P<0.05$, **$P<0.01$, ***$P<0.001$. Treatment with C646 (3 μmol/L) significantly reduced VCAM-1 levels in the cultured endothelial cells (n=3 mice). Mean±SEM; *$P<0.05$. DAPI, 4′,6-diamidino-2-phenylindole; eNOS indicates endothelial nitric oxide synthase; IB4, isolectin B4; SIRT3, sirtuin 3; SIRT3KO, SIRT3 knockout; and VCAM-1, vascular cell adhesion molecule 1; and WT, wild type.

coronary conditions at all levels, either improvement of the coronary artery or microcirculation (capillaries) would lead to increased CFR.[2] Our data that knockout of SIRT3 resulted in increased thickness of arteries and that was not significantly suppressed in SIRT3KO mice+C646, indicating that C646-induced improvement of CFR was not due to its effect on the remodeling of large vessels. Accumulating evidence suggests that microvascular dysfunction including endothelial inflammation, eNOS uncoupling, and capillaries rarefaction
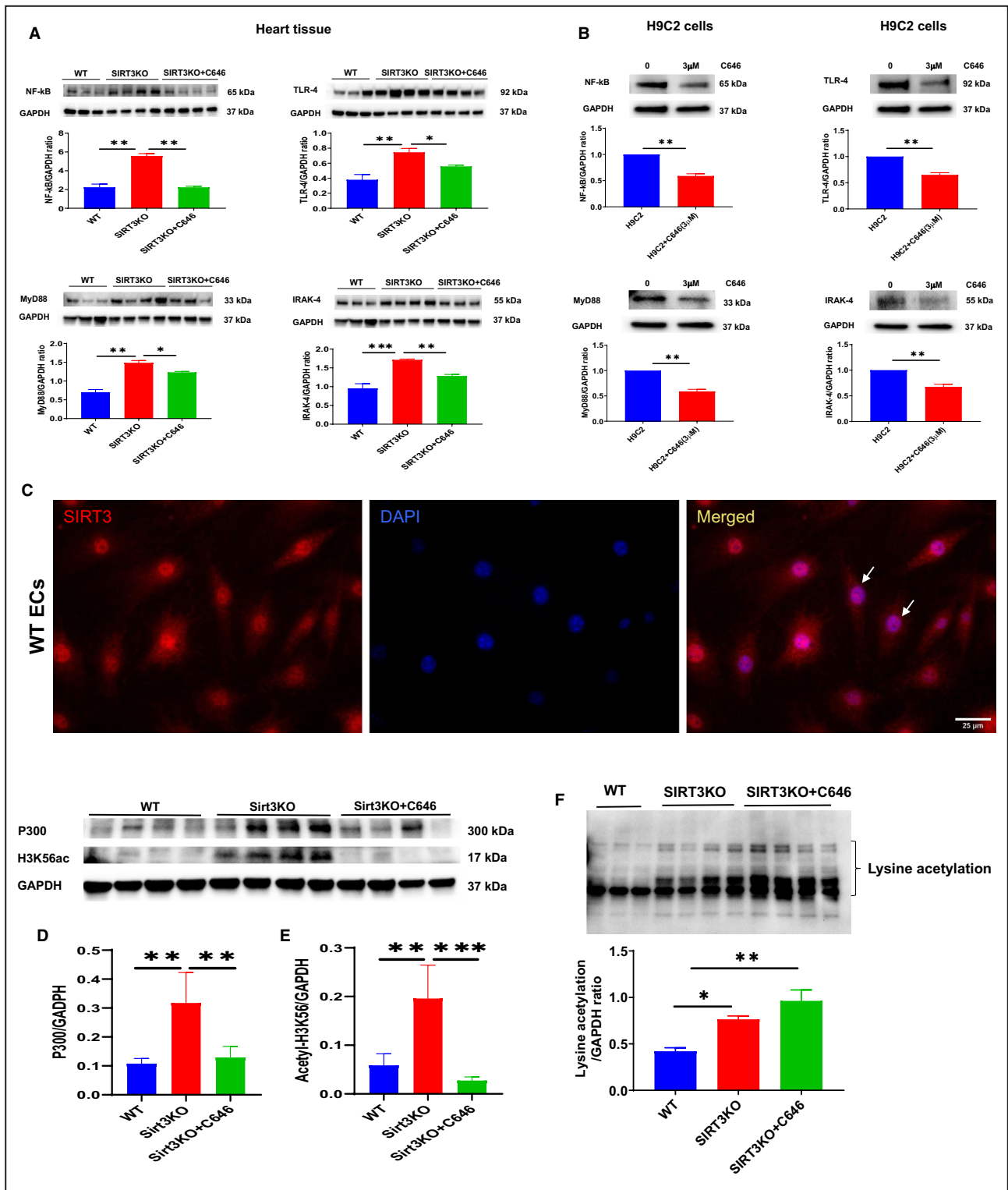
causes impaired CFR,[1–3,10] among which endothelial dysfunction plays a significant role.[7,9] Thus, the improvement of endothelial dysfunction could enhance CFR. Our study showed that treatment with C646 significantly reversed the down-regulation of eNOS expression in the SIRT3KO mice and increased the eNOS levels in the cultured ECs. It is well known that

eNOS is essential for the maintenance of endothelial function, and the uncoupling of eNOS will result in less release of nitric oxide, leading to endothelial dysfunction.[41,42] C646 may ameliorate endothelial dysfunction via up-regulating eNOS expression, which subsequently improved CFR. We also found that treatment with C646 attenuated microvascular rarefaction in the

Figure 6. Treatment with C646 reduced expression of NF-κB and associated factors in SIRT3KO mice.
A, Knockout of SIRT3 increased the expression of NF-κB, TLR-4, MyD88, and IRAK-4 in the mouse hearts (n=4 mice). This increase was reversed by treatment with C646 (n=3–4 mice). Mean±SEM; *P<0.05, **P<0.01, ***P<0.001. **B**, Treatment with C646 (3 μmol/L) significantly reduced the basal levels of NF-κB, TLR-4, MyD88, and IRAK-4 in the H9C2 cell lines (n=3 cell lines). Mean±SEM; **P<0.01. **C**, Immunofluorescence analyses of SIRT3 localization in the cultured ECs using an antibody specific to SIRT3. DAP1 was used to visualize the nuclei. The SIRT3 antibodies recognized a protein that resided exclusively in the nucleus that was colocalized with the blue DAPI regions (white arrow). **D**, Western blot analysis showed that knockout of SIRT3 resulted in a significant increase in p300 expression in the mouse hearts. C646 treatment significantly reduced the levels of p300 in the SIRT3KO mice (n=4 mice, **P<0.01). **E**, Western blot analysis showed that knockout of SIRT3 led to a significant increase in H3K56 acetylation. C646 treatment significantly attenuated the acetylated H3K56 levels in the hearts of SIRT3KO mice (n=4 mice, **P<0.01, ***P<0.001). **F**, Western blot analysis showed that knockout of SIRT3 resulted in a significant increase in total lysine acetylation in the mouse hearts.C646 treatment had little effect on total lysine acetylation levels in the SIRT3KO mice (n=3–4 mice, *P<0.05, **P<0.01). DAPI indicates 4′,6-diamidino-2-phenylindole; ECs, endothelial cells; H3K56 acetylation, acetyl-histone H3 (lys56); IRAK-4, interleukin-1 receptor-associated kinase 4; MyD88, myeloid differentiation primary response 88; NF-κB, nuclear factor kappa-light-chain-enhancer of activated B cells; SIRT3, sirtuin 3; SIRT3KO, SIRT3 knockout; TLR-4, toll-like receptor 4; and WT, wild type.

SIRT3KO mice, which may contribute to the improvement of CFR.[3,10] Previous studies revealed that both hypertrophy and fibrosis are associated with microvascular rarefaction and reduced CFR.[1,32–35] We also observed a significant reduction of hypertrophy and fibrosis in the SIRT3KO mice following the C646 treatment, which partly explains the amelioration of CFR in the SIRT3KO mice. Taken together, our data indicate that C646 treatment enhances CFR in SIRT3KO mice via ameliorating microvascular rarefaction and cardiac remodeling, which may be associated with improvement of cardiac function. In addition, arterial stiffening has been strongly suggested to be associated with impaired CFR and cardiac performance in both preclinical and clinical studies. Our present study showed that PWV was significantly increased in the SIRT3KO mice. Treatment of C646 resulted in a significant improvement of arterial stiffness. This may also be potentially responsible for the improved CFR and cardiac performance by C646 treatment, which is independent of changes in the coronary microvascular circulation.

An imbalanced arginase/eNOS in favor of arginase has been contributed to endothelial dysfunction.[41–45] Arginase has 2 isoforms: arginase I and arginase II. Arginase I is cytoplasmic and mainly expressed in the liver, whereas arginase II is mitochondrial and mainly expressed in the kidney and heart. Both of these could compete with eNOS for L-arginine, resulting in eNOS uncoupling. The uncoupling of eNOS not only reduces nitric oxide production but also increases oxidative stress and inflammatory responses.[42,45–49] For the first time, we demonstrated that knockout of SIRT3 up-regulated arginase II expression together with an increased arginase activity in the mouse heart. Treatment with C646 significantly reduced arginase II expression and inhibited arginase activity in the SIRT3KO mice. Interestingly, arginase I was not affected by the knockout of SIRT3 and C646 treatment, suggesting that mitochondrial arginase II was the main contributor to the increased arginase activity in the heart. Our data further confirmed that C646 reduced the expression of arginase II in the cultured ECs. Inhibition of arginase II

expression and activity by C646 could rebalance arginase/eNOS and promote eNOS activity, which may be associated with the amelioration of ROS formation and VCAM-1 expression shown in our present study[42,45,47–49] and may also contribute to improvements of endothelial dysfunction and microvascular rarefaction.[34,45,48]

NF-κB is a family of transcription factors responsible for immune responses and proinflammation.[50] The NF-κB-mediated inflammatory response has contributed to the pathogenesis of myocardial fibrosis and hypertrophy.[51–55] Our present study demonstrated that NF-κB expression was significantly inhibited by treatment with C646 in the hearts of SIRT3KO mice. In the cultured H9C2 cell lines, C646 also suppressed NF-κB expression, further confirming the inhibitory role of C646 on NF-κB-induced inflammation. To further examine NF-κB-mediated inflammatory response, we measured the expressions of TLR-4, IRAK-4, and MyD88, which are defined as regulators of NF-κB and are innate immune.[54,56,57] Our data showed that knockout of SIRT3 increased levels of TLR-4, IRAK-4, and MyD88, whereas C646 treatment blunted this up-regulation in the mouse hearts. The same inhibitory effects of C646 on the expression of TLR-4, IRAK-4, and MyD88 were validated in the cultured H9C2 cell lines. These results indicate that C646 treatment reverses inflammatory responses in the SIRT3KO mice through suppressing NF-κB, contributing to the alleviation of cardiac fibrosis and hypertrophy.

In addition to its well-recognized roles in mitochondrial function, SIRT3 also exhibits a previously unappreciated role in the nucleus.[19,20,58–60] SIRT3 has been shown to be capable of histone deacetylase activity against H3K9ac (acetylated histone H3 lysine 9) and H4K16ac in vivo.[19,20] SIRT3 also regulates the expression of nuclear genes, such as *PGC-1α* and *Mn-SOD*, and directly modulates the activity of the FOXO3A transcription factor by deacetylation.[59,60] These studies suggest that SIRT3 may exhibit a functional role outside mitochondria through its histone deacetylase activity. Consistent with these findings, our present

study demonstrated that SIRT3 resided in the nuclei of cultured mouse ECs. Furthermore, knockout of SIRT3 significantly increased levels of p300 and H3K56 acetylation in vivo. Importantly, C646 treatment significantly attenuated SIRT3KO-mediated p300 expression and H3K56 acetylation. Taken together, our present study provided a novel role of the SIRT3–p300 HAT pathway in mediating CMD and heart failure.

This study had some limitations. First, we did not examine whether and how SIRT3 affects nuclear p300 and H3K56 acetylation. However, our study suggests a novel role of p300 HAT inhibitor in SIRT3KO-mediated CMD and cardiac remodeling. Although our data showed an increase in the expression of lysine acetylation in the hearts of SIRT3KO mice, we did not actually measure the levels of mitochondrial acetylation as well as nuclear acetylation. Further studies are warranted to further explore the potential retrograde signaling of mitochondria on p300 and H3K56 acetylation in the nuclei.

In conclusion, our current work demonstrated a potential therapeutic role of C646, a p300 HAT inhibitor, on CMD and cardiac dysfunction. C646 treatment significantly attenuates p300 expression and H3K56 acetylation and improves CFR, arterial stiffness, and cardiac performance by the mechanisms involving in inhibition of endothelial dysfunction and NF-κB-mediated inflammation.

REFERENCES

1. Bradley AJ, Alpert JS. Coronary flow reserve. *Am Heart J*. 1991; 122:1116–1128.
2. Gan LM, Wikstrom J, Fritsche-Danielson R. Coronary flow reserve from mouse to man–from mechanistic understanding to future interventions. *J Cardiovasc Transl Res*. 2013;6:715–728.
3. Kaul S, Jayaweera AR. Myocardial capillaries and coronary flow reserve. *J Am Coll Cardiol*. 2008;52:1399–1401.
4. Shantouf RS, Mehra A. Coronary fractional flow reserve. *Am J Roentgenol*. 2015;204:W261–W265.
5. Murthy VL, Naya M, Foster CR, Gaber M, Hainer J, Klein J, Dorbala S, Blankstein R, Di Carli MF. Association between coronary vascular dysfunction and cardiac mortality in patients with and without diabetes mellitus. *Circulation*. 2012;126:1858–1868.
6. Schalkwijk CG, Stehouwer CD. Vascular complications in diabetes mellitus: the role of endothelial dysfunction. *Clin Sci*. 2005;109:143–159.
7. Oflaz H, Sen F, Bayrakli SK, Elitok A, Cimen AO, Golcuk E, Kasikcioglu E, Tukenmez M, Yazici H, Turkmen A. Reduced coronary flow reserve and early diastolic filling abnormalities in patients with nephrotic syndrome. *Ren Fail*. 2008;30:914–920.
8. Gould KL, Johnson NP, Bateman TM, Beanlands RS, Bengel FM, Bober R, Camici PG, Cerqueira MD, Chow BJW, Di Carli MF, et al. Anatomic versus physiological assessment of coronary artery disease. Role of coronary flow reserve, fractional flow reserve, and positron emission tomography imaging in revascularization decision-making. *J Am Coll Cardiol*. 2013;62:1639–1653.
9. Knecht M, Burkhoff D, Yi GH, Popilskis S, Homma S, Packer M, Wang J. Coronary endothelial dysfunction precedes heart failure and reduction of coronary reserve in awake dogs. *J Mol Cell Cardiol*. 1997;29:217–227.
10. Zeng H, Chen JX. Microvascular rarefaction and heart failure with preserved ejection fraction. *Front Cardiovasc Med*. 2019;6:15.
11. Ahn BH, Kim HS, Song S, Lee IH, Liu J, Vassilopoulos A, Deng CX, Finkel T. A role for the mitochondrial deacetylase Sirt3 in regulating energy homeostasis. *Proc Natl Acad Sci USA*. 2008;105:14447–14452.
12. Haigis MC, Deng CX, Finley LW, Kim HS, Gius D. Sirt3 is a mitochondrial tumor suppressor: a scientific tale that connects aberrant cellular ROS, the Warburg effect, and carcinogenesis. *Cancer Res*. 2012;72:2468–2472.
13. Zeng H, Vaka VR, He X, Booz GW, Chen JX. High-fat diet induces cardiac remodeling and dysfunction: assessment of the role played by SIRT3 loss. *J Cell Mol Med*. 2015;19:1847–1856.
14. Lin CC, Yang CC, Wang CY, Tseng HC, Pan CS, Hsiao LD, Yang CM. NADPH oxidase/ROS-dependent VCAM-1 induction on TNF-alpha-challenged human cardiac fibroblasts enhances monocyte adhesion. *Front Pharmacol*. 2015;6:310.
15. He X, Zeng H, Chen JX. Emerging role of sirt3 in endothelial metabolism, angiogenesis, and cardiovascular disease. *J Cell Physiol*. 2019;234:2252–2265.
16. He X, Zeng H, Chen JX. Ablation of SIRT3 causes coronary microvascular dysfunction and impairs cardiac recovery post myocardial ischemia. *Int J Cardiol*. 2016;215:349–357.
17. Sundaresan NR, Bindu S, Pillai VB, Samant S, Pan Y, Huang JY, Gupta M, Nagalingam RS, Wolfgeher D, Verdin E, et al. Sirt3 blocks aging-associated tissue fibrosis in mice by deacetylating and activating glycogen synthase kinase 3beta. *Mol Cell Biol*. 2015;36:678–692.
18. Dou C, Liu Z, Tu K, Zhang H, Chen C, Yaqoob U, Wang Y, Wen J, van Deursen J, Sicard D, et al. P300 acetyltransferase mediates stiffness-induced activation of hepatic stellate cells into tumor-promoting myofibroblasts. *Gastroenterology*. 2018;154:2209–2221.e14.
19. Iwahara T, Bonasio R, Narendra V, Reinberg D. Sirt3 functions in the nucleus in the control of stress-related gene expression. *Mol Cell Biol*. 2012;32:5022–5034.
20. Scher MB, Vaquero A, Reinberg D. Sirt3 is a nuclear nad+-dependent histone deacetylase that translocates to the mitochondria upon cellular stress. *Genes Dev*. 2007;21:920–928.
21. Liu CF, Tang WHW. Epigenetics in cardiac hypertrophy and heart failure. *JACC Basic Transl Sci*. 2019;4:976–993.
22. Wang Y, Miao X, Liu Y, Li F, Liu Q, Sun J, Cai L. Dysregulation of histone acetyltransferases and deacetylases in cardiovascular diseases. *Oxid Med Cell Longev*. 2014;2014:641979.
23. Vempati RK, Jayani RS, Notani D, Sengupta A, Galande S, Haldar D. P300-mediated acetylation of histone h3 lysine 56 functions in DNA damage response in mammals. *J Biol Chem*. 2010;285:28553–28564.
24. He X, Zeng H, Chen ST, Roman RJ, Aschner JL, Didion S, Chen JX. Endothelial specific SIRT3 deletion impairs glycolysis and angiogenesis and causes diastolic dysfunction. *J Mol Cell Cardiol*. 2017;112:104–113.
25. Su H, Zeng H, Liu B, Chen J-X. Sirtuin 3 is essential for hypertension-induced cardiac fibrosis via mediating pericyte transition. *J Cell Mol Med*. 2020;24:8057–8068.

26. Zeng H, He X, Chen JX. Endothelial sirtuin 3 dictates glucose transport to cardiomyocyte and sensitizes pressure overload-induced heart failure. *J Am Heart Assoc*. 2020;9:e015895. DOI: 10.1161/JAHA.120.015895.

27. Bugyei-Twum A, Advani A, Advani SL, Zhang Y, Thai K, Kelly DJ, Connelly KA. High glucose induces Smad activation via the transcriptional coregulator p300 and contributes to cardiac fibrosis and hypertrophy. *Cardiovasc Diabetol*. 2014;13:89.

28. Morimoto T, Sunagawa Y, Kawamura T, Takaya T, Wada H, Nagasawa A, Komeda M, Fujita M, Shimatsu A, Kita T, et al. The dietary compound curcumin inhibits p300 histone acetyltransferase activity and prevents heart failure in rats. *J Clin Invest*. 2008;118:868–878.

29. Bezzerides VJ, Platt C, Lerchenmuller C, Paruchuri K, Oh NL, Xiao C, Cao Y, Mann N, Spiegelman BM, Rosenzweig A. Cited4 induces physiologic hypertrophy and promotes functional recovery after ischemic injury. *JCI Insight*. 2016;1:e85904.

30. Rubio K, Singh I, Dobersch S, Sarvari P, Gunther S, Cordero J, Mehta A, Wujak L, Cabrera-Fuentes H, Chao CM, et al. Inactivation of nuclear histone deacetylases by ep300 disrupts the micee complex in idiopathic pulmonary fibrosis. *Nat Commun*. 2019;10:2229.

31. Rai R, Sun T, Ramirez V, Lux E, Eren M, Vaughan DE, Ghosh AK. Acetyltransferase p300 inhibitor reverses hypertension-induced cardiac fibrosis. *J Cell Mol Med*. 2019;23:3026–3031.

32. Gogiraju R, Xu X, Bochenek ML, Steinbrecher JH, Lehnart SE, Wenzel P, Kessel M, Zeisberg EM, Dobbelstein M, Schafer K. Endothelial p53 deletion improves angiogenesis and prevents cardiac fibrosis and heart failure induced by pressure overload in mice. *J Am Heart Assoc*. 2015;4:e001770. DOI: 10.1161/JAHA.115.001770.

33. Krams R, Kofflard MJ, Duncker DJ, Von Birgelen C, Carlier S, Kliffen M, ten Cate FJ, Serruys PW. Decreased coronary flow reserve in hypertrophic cardiomyopathy is related to remodeling of the coronary microcirculation. *Circulation*. 1998;97:230–233.

34. Mohammed SF, Hussain S, Mirzoyev SA, Edwards WD, Maleszewski JJ, Redfield MM. Coronary microvascular rarefaction and myocardial fibrosis in heart failure with preserved ejection fraction. *Circulation*. 2015;131:550–559.

35. Morine KJ, Qiao X, York S, Natov PS, Paruchuri V, Zhang Y, Aronovitz MJ, Karas RH, Kapur NK. Bone morphogenetic protein 9 reduces cardiac fibrosis and improves cardiac function in heart failure. *Circulation*. 2018;138:513–526.

36. Inuzuka H, Gao D, Finley LW, Yang W, Wan L, Fukushima H, Chin YR, Zhai B, Shaik S, Lau AW, et al. Acetylation-dependent regulation of skp2 function. *Cell*. 2012;150:179–193.

37. Pozzi A, Moberg PE, Miles LA, Wagner S, Soloway P, Gardner HA. Elevated matrix metalloprotease and angiostatin levels in integrin alpha 1 knockout mice cause reduced tumor vascularization. *Proc Natl Acad Sci USA*. 2000;97:2202–2207.

38. He X, Zeng H, Roman RJ, Chen JX. Inhibition of prolyl hydroxylases alters cell metabolism and reverses pre-existing diastolic dysfunction in mice. *Int J Cardiol*. 2018;272:281–287.

39. Tang M, Huang Z, Luo X, Liu M, Wang L, Qi Z, Huang S, Zhong J, Chen JX, Li L, et al. Ferritinophagy activation and sideroflexin1-dependent mitochondria iron overload is involved in apelin-13-induced cardiomyocytes hypertrophy. *Free Radic Biol Med*. 2019;134:445–457.

40. Hou X, Zeng H, He X, Chen JX. Sirt3 is essential for apelin-induced angiogenesis in post-myocardial infarction of diabetes. *J Cell Mol Med*. 2015;19:53–61.

41. Johnson FK, Peyton KJ, Liu XM, Azam MA, Shebib AR, Johnson RA, Durante W. Arginase promotes endothelial dysfunction and hypertension in obese rats. *Obesity (Silver Spring)*. 2015;23:383–390.

42. Vanhoutte PM. Arginine and arginase: endothelial no synthase double crossed? *Circ Res*. 2008;102:866–868.

43. Koo BH, Hwang HM, Yi BG, Lim HK, Jeon BH, Hoe KL, Kwon YG, Won MH, Kim YM, Berkowitz DE, et al. Arginase ii contributes to the ca(2+)/camkii/enos axis by regulating ca(2+) concentration between the cytosol and mitochondria in a p32-dependent manner. *J Am Heart Assoc*. 2018;7:e009579. DOI: 10.1161/JAHA.118.009579.

44. Krause BJ, Del Rio R, Moya EA, Marquez-Gutierrez M, Casanello P, Iturriaga R. Arginase-endothelial nitric oxide synthase imbalance contributes to endothelial dysfunction during chronic intermittent hypoxia. *J Hypertens*. 2015;33:515–524; discussion 524.

45. Berkowitz DE, White R, Li D, Minhas KM, Cernetich A, Kim S, Burke S, Shoukas AA, Nyhan D, Champion HC, et al. Arginase reciprocally regulates nitric oxide synthase activity and contributes to endothelial dysfunction in aging blood vessels. *Circulation*. 2003;108:2000–2006.

46. Caldwell RW, Rodriguez PC, Toque HA, Narayanan SP, Caldwell RB. Arginase: a multifaceted enzyme important in health and disease. *Physiol Rev*. 2018;98:641–665.

47. Yepuri G, Velagapudi S, Xiong Y, Rajapakse AG, Montani JP, Ming XF, Yang Z. Positive crosstalk between arginase-II and S6K1 in vascular endothelial inflammation and aging. *Aging Cell*. 2012;11:1005–1016.

48. Paulus WJ, Tschope C. A novel paradigm for heart failure with preserved ejection fraction: comorbidities drive myocardial dysfunction and remodeling through coronary microvascular endothelial inflammation. *J Am Coll Cardiol*. 2013;62:263–271.

49. Liang X, Arullampalam P, Yang Z, Ming XF. Hypoxia enhances endothelial intercellular adhesion molecule 1 protein level through upregulation of arginase type II and mitochondrial oxidative stress. *Front Physiol*. 2019;10:1003.

50. Javan H, Szucsik AM, Li L, Schaaf CL, Salama ME, Selzman CH. Cardiomyocyte p65 nuclear factor-kappab is necessary for compensatory adaptation to pressure overload. *Circ Heart Fail*. 2015;8:109–118.

51. Johar S, Cave AC, Narayanapanicker A, Grieve DJ, Shah AM. Aldosterone mediates angiotensin ii-induced interstitial cardiac fibrosis via a Nox2-containing NADPH oxidase. *FASEB J*. 2006;20:1546–1548.

52. Ogata T, Miyauchi T, Sakai S, Takanashi M, Irukayama-Tomobe Y, Yamaguchi I. Myocardial fibrosis and diastolic dysfunction in deoxycorticosterone acetate-salt hypertensive rats is ameliorated by the peroxisome proliferator-activated receptor-alpha activator fenofibrate, partly by suppressing inflammatory responses associated with the nuclear factor-kappa-b pathway. *J Am Coll Cardiol*. 2004;43:1481–1488.

53. Thirugnanam K, Cossette SM, Lu Q, Chowdhury SR, Harmann LM, Gupta A, Spearman AD, Sonin DL, Bordas M, Kumar SN, et al. Cardiomyocyte-specific SNRK prevents inflammation in the heart. *J Am Heart Assoc*. 2019;8:e012792. DOI: 10.1161/JAHA.119.012792.

54. Ma D, Zhang J, Zhang Y, Zhang X, Han X, Song T, Zhang Y, Chu L. Inhibition of myocardial hypertrophy by magnesium isoglycyrrhizinate through the tlr4/nf-kappab signaling pathway in mice. *Int Immunopharmacol*. 2018;55:237–244.

55. Zhao QD, Viswanadhapalli S, Williams P, Shi Q, Tan C, Yi X, Bhandari B, Abboud HE. Nadph oxidase 4 induces cardiac fibrosis and hypertrophy through activating akt/mtor and nfkappab signaling pathways. *Circulation*. 2015;131:643–655.

56. Echavarria R, Mayaki D, Neel JC, Harel S, Sanchez V, Hussain SN. Angiopoietin-1 inhibits toll-like receptor 4 signalling in cultured endothelial cells: Role of mir-146b-5p. *Cardiovasc Res*. 2015;106:465–477.

57. Zhong L, Simard MJ, Huot J. Endothelial micrornas regulating the nf-kappab pathway and cell adhesion molecules during inflammation. *FASEB J*. 2018;32:4070–4084.

58. Shi T, Wang F, Stieren E, Tong Q. Sirt3, a mitochondrial sirtuin deacetylase, regulates mitochondrial function and thermogenesis in brown adipocytes. *J Biol Chem*. 2005;280:13560–13567.

59. Sundaresan NR, Gupta M, Kim G, Rajamohan SB, Isbatan A, Gupta MP. Sirt3 blocks the cardiac hypertrophic response by augmenting foxo3a-dependent antioxidant defense mechanisms in mice. *J Clin Invest*. 2009;119:2758–2771.

60. Sundaresan NR, Samant SA, Pillai VB, Rajamohan SB, Gupta MP. Sirt3 is a stress-responsive deacetylase in cardiomyocytes that protects cells from stress-mediated cell death by deacetylation of ku70. *Mol Cell Biol*. 2008;28:6384–6401.